University of Ljubljana

J. Stefan Institute, Ljubljana, Slovenia

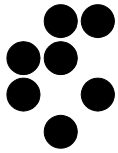

Report **DP-7260**

Measurements and mathematical modelling of a semi-industrial liquid-gas separator for the purpose of fault diagnosis

Damir Vrančić

Đani Juričić

Janko Petrovčič

August 1995

COPERNICUS PROJECT CT94-02337

TITLE:	**Semi-industrial benchmark problem: measurements and mathematical modelling of a process for separation gas from liquid**
SOURCE:	Jozef Stefan Institute
STATUS:	Issue A
AUTHORS:	Damir Vrančić, Đani Juričić, Janko Petrovčič
DISTRIBUTION:	All partners
DATE:	Aug 22, 1995
NUMBER OF PAGES:	48
INTERNAL REFERENCE:	COPL002R
COPERNICUS WORKPACKAGE:	WP2

Abstract:

Gas-liquid separation process is one of the benchmark processes which will be used for testing and evaluation of various fault detection and isolation methods. This process unit makes part of a semi-industrial plant serving for pilot studies in NO_x reduction in flue gasses and wastewater treatment.

The process consists of high quality components and instrumentation and is built up according to industrial standards. This fact contributed to the final model quality particularly through reliable and “pure” (i.e. low-noise) measurements.

In this work a non-linear dynamic model of the process is developed and validated at different working conditions. An interesting property of the process is that the steady-state values of one of the process outputs are very sensitive to the changes in steady-state values of process inputs. The implication is that in the feasible working range the process shows near-integral behaviour. However, the results of experiments show that the model satisfactory describes the process dynamics.

Experimental results obtained at different working conditions and artificially injected faults are presented and discussed. The corresponding data records are documented in ASCII files.

Table of contents

1. Process description

Separation gas from liquid refers to a subprocess within the semi-industrial installation which is used for reduction of NO_x in effluent gasses and technological waste water treatment by means of neutralisation with CO_2 contained in flue gasses. The role of the separation unit is to capture flue gasses under low pressure from effluent channels by means of water flow and to carry them over under high enough pressure to the further (neutralisation) stage. The separation unit is shown in Fig. 1.

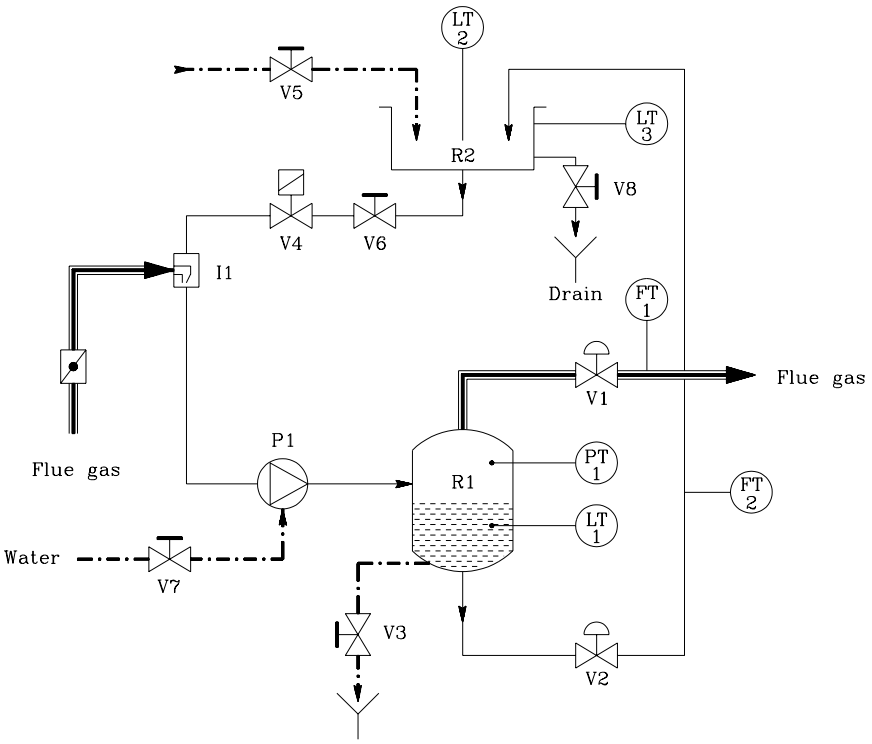

Fig. 1. Process scheme of the separation unit

The flue gasses coming from the effluent channels are "pooled" by the water flow into the water circulation pipe through the injector I_1. The water flow is generated by the pump P_1 (water ring). Speed of the pump is kept constant. The pump feeds the mixture of water and gas into the separator R_1 where gas is separated from water. Hence the accumulated gas in R_1 forms a sort of "gas cushion" with increased internal pressure. Owing to this pressure, flue gas is blown out from R_1 into the next neutralisation unit. On the other side the "cushion" forces water to circulate back to

the reservoir R_2. The quantity of water in the circuit is constant. If from this or that reason additional water is needed, the water supply path through the valve V_5 is utilised.

Table 1 shows the list of all process components.

The used constants and variables are given in appendix 1.

Symbol	***Description***
R_1	Gas-liquid separator
R_2	Reservoir (opened at the top)
I_1	Gas injector
P_1	Electric pump
V_1	Main gas valve from the separator
V_2	Main liquid valve from the separator
V_3	Manual valve producing leak in R_1 (for fault detection purposes)
V_4	Electromagnetic valve (open during the experiments)
V_5	Manual valve for feeding additional water into R_2
V_6	Manual valve
V_7	Manual valve for feeding additional water into the water pump P_1.
V_8	Manual valve producing leak in R_2 (for fault detection purposes)
PT_1	Gas pressure sensor in R_1
LT_1	Liquid level sensor in R_1
LT_2	Liquid level sensor in R_2
LT_3	ON/OFF level sensor in R_2
FT_1	Gas flow-meter
FT_2	Liquid flow-meter

Table 1. List of process components

1.1 Transmitters

Table 2 lists the transmitters used in the system.

Symbol	*Variable*	*Unit*	*Range*	*Description*
PT_1	p_1	bar	0..1	Pressure inside the separator R_1 *above* the normal atmospheric pressure
LT_1	h_1	m	0..2	Water level inside the separator R_1 measured by Δp sensor
LT_2	h_2	m	0..1	Water level inside the reservoir R_2 measured by Δp sensor
LT_3	-	-	ON/OFF	The on/off water level sensor (security)
FT_1	Φ_1	l/s	1.5..20	The volumetric air flow from the separator R_1
FT_2	Φ_2	l/s	0.03..0.5	The volumetric water flow from the separator R_1

Table 2. List of transmitters

Pressure transmitter PT_1 is PMC 133 from *Endress+Hauser*, pressure transmitters for measuring levels LT_1 and LT_2 are 3051 CD from *Rosemount*, LT_3 is LIQUIPHANT FTL 160 from *Endress+Hauser* and the flow meters FT_1 and FT_2 are SWINGWIRL II DMV 6331 from *Endress+Hauser*.

1.2 Actuators

Table 3 lists the actuators used in the system.

The valve V_1 is 6 713 341 DN 32 from *Eckardt* and valve V_2 is 6 713 221 DN 15 from *Eckardt*. The electromagnetic valve V_4 is type M1T8 from *Stäfa Control Systems AG* and motor of the pump P_1 is type SEVER OB 11/4-II from *Litostroj*.

Symbol	*Variable*	*Unit*	*Range*	*Description*
V_1	u_1	-	0..1	The equal-percentage servo valve for controlling the gas flow from the separator. The value of the variable u_1=0 implies closed valve and the value u_1=1 implies fully-opened valve[1].
V_2	u_2	-	0..1	The equal-percentage servo valve for controlling the liquid flow from the separator. The value of the variable u_2=0 implies closed valve and the value u_2=1 implies fully-opened valve[1].
V_4	-	-	on/off	The electromagnetic valve V_4. Fully opened during experiment.
P_1	-	-	-	The pump. It runs with constant (full) speed and is driven by asynchronous motor of rated power P=1.8 kW.

Table 3. List of actuators

1.3 Signals

The following measured signals are available in the system:

Variable	*Description*
h_1	water level in the separator R_1
h_2	water level in the reservoir R_2
-	ON/OFF level sensor in the reservoir R_2
p_1	gas pressure in R_1
Φ_1	gas flow on the outlet of the unit
Φ_2	water flow on the outlet of R_1
u_1	signal on the continuous valve 1
u_2	signal on the continuous valve 2

Table 4. List of measured signals

[1] Valves V_1 and V_2 are actually driven by current signals in the range of 4..20mA. For easier manipulation we use the relative range 0..1. u=0 corresponds to 4mA current and u=1 corresponds to 20mA current.

2. Derivation of the non-linear dynamic model

Fig. 2. shows a more detailed scheme of the unit for separation.

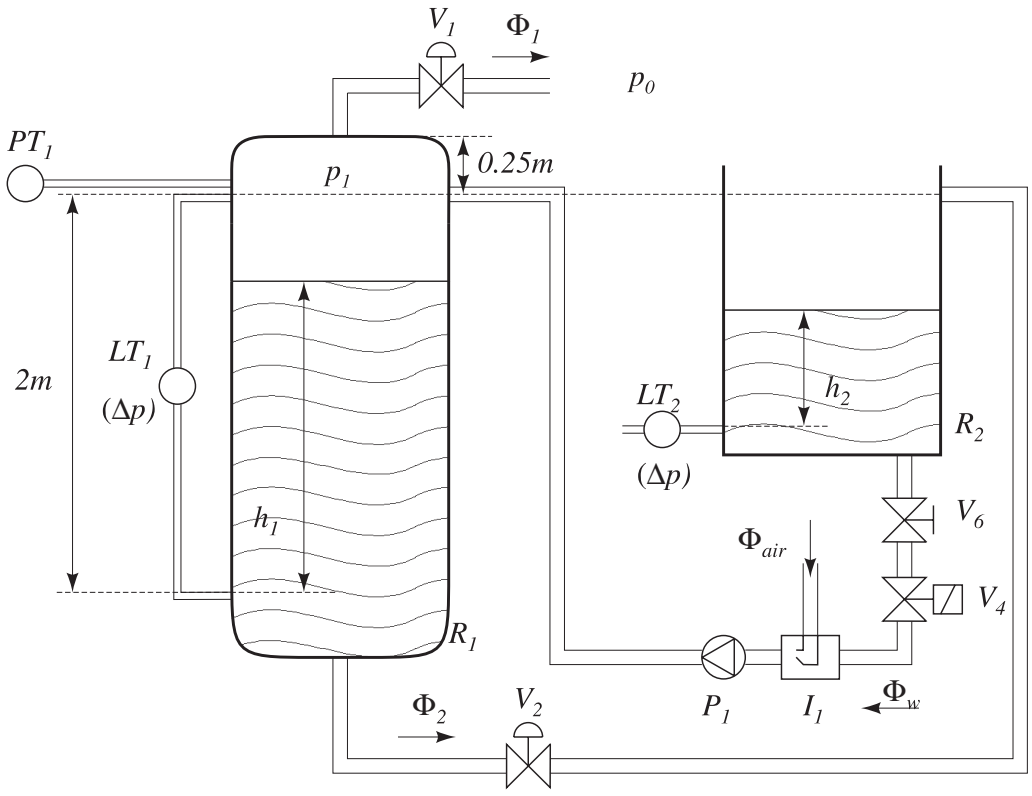

Fig. 2. Gas-liquid separator unit

Variable p_1 denotes the gas pressure above the normal atmospheric pressure inside the separator R_1, h_1 and h_2 are measured water levels (by Δp sensors) in R_1 and R_2, respectively. Φ_{air} and Φ_w are air and water flows to R_1.

2.1 Modelling the valves

Firstly, we tried to find the model of two continuous valves V_1 and V_2.

Valve characteristics are usually modelled by the non-linear expression [2]:

$$\Phi = K\sqrt{\Delta p} \tag{1}$$

where Φ, K and Δp are flow through the valve, valve flow coefficient and the difference of the pressure on both sides of the valve, respectively. Valves used in our case are *equal-percentage* valves. Main characteristic of such valves is that K is an exponential function of the valve command signal [2]:

$$K = K_{\max} R^{v-1} \tag{2}$$

where v, K_{max} and R denote valve position (v=0 denotes fully closed and v=1 denotes fully opened valve), the K of the fully opened valve (v=1) and the K_{max}/K_{min} ratio (K_{min} denotes the K of the minimum opened valve (v=0)), respectively.

Both valves are driven by servo motors. The actual input signal to the valve is current signal in the range of 4..20 mA which is linearly transformed into the range u=0..1 for easier manipulation. This command signal serves as reference for the valve position (v) (in the steady-state v=u). More detailed explanation can be found in subsections 2.1.1 and 2.1.2.

2.1.1 Valve V_1

The static characteristic of the first valve (V_1) was obtained by measuring the valve command signal (u_1), which is the reference for the valve position v_1, and flow through the valve (Φ_1) at different gas pressures in the separator. Table 5 presents the obtained measurements.

We used the valve command signal (u_1) only in the range between u_1=0.33 to u_1=0.66. Smaller values were not used because in that case pressure p_1 would increase too much. At higher values of u_1 pressure p_1 decreases too much and, as a consequence, accurate values of K_1 can not be obtained.

First, we calculated the flow coefficient K_1 at different values u_1 from equation (1):

$$K_1 = \frac{\Phi_1}{\sqrt{p_1}}\ , \tag{3}$$

where p_1 represents the excess of pressure *above* the normal atmospheric pressure p_0.

p_1 [bar]	u_1 [-]	Φ_1 [l/s]
0.8	0.33	4.92
0.7	0.357	5.24
0.6	0.381	5.54
0.5	0.413	5.75
0.4	0.447	5.92
0.3	0.492	5.94
0.2	0.55	6.02
0.1	0.66	6.27

Table 5: Measurements on the first valve

The resulting flow coefficient K_1 at different u_1, calculated from Table 2 and expression (3), is given in Table 6.

u_1 [-]	$K_1 \left[\frac{l}{s\sqrt{bar}} \right]$
0.33	5.5
0.357	6.263
0.381	7.835
0.413	8.132
0.447	9.36
0.492	10.845
0.55	13.46
0.66	19.83

Table 6: K_1 vs. u_1

Appropriate constants K_{max} and R were found by logarithming the expression (2) and using the least squares solution. When taking into account the fact that in steady-state $v_1=u_1$, the result of the estimated flow coefficient is:

$$K_1 = K_{01} \cdot R_1^{\,v_1 - 1} = 75.1 \cdot 46.1^{v_1 - 1} \left[\frac{l}{s\sqrt{bar}} \right] \tag{4}$$

Fig. 3 shows the difference between measurements (marked with asterisk) and the estimated function (4).

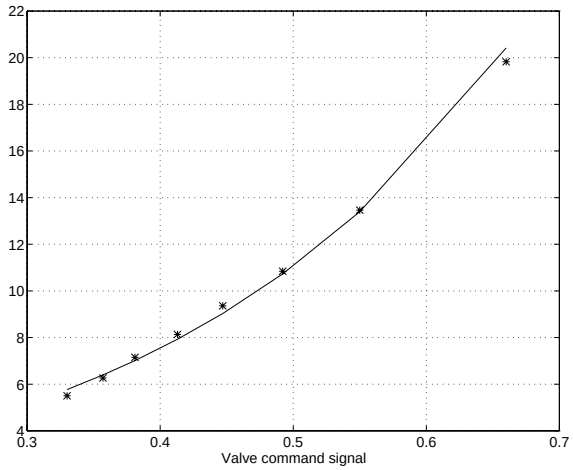

*Fig. 3. Static characteristic of the valve V_1: flow coefficient K_1 vs. valve command signal u_1; * measurements, __ model*

The static characteristics must be extended by dynamic relationship between the command signal u and actual valve position v. Namely, the head of the valve needs some time to reach the desired position due to the servo-mechanism. In fact, valve position v can be changed only with limited speed, i.e.:

$$\dot{v} = \begin{cases} \dot{v}_{\max} & if \ \dot{u} > \dot{v}_{\max} \\ \dot{v}_{\min} & if \ \dot{u} < \dot{v}_{\min} \\ \dot{u} & otherwise \end{cases} \tag{5}$$

where $\dot{v}_{\max}$ =0.66 s^{-1} and $\dot{v}_{\min}$ =-0.33 s^{-1}. Hence the entire valve model is as shown in Fig. 4.

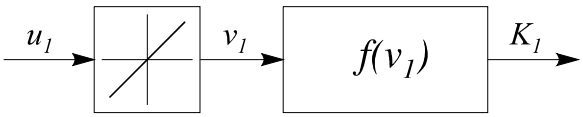

Fig. 4. The entire valve model

2.1.2 Valve V_2

The characteristic of the second valve was obtained from measurements of the valve command signal (u_2), flow through the valve (Φ_2) and water level h_1. All measurements were obtained at constant pressure p_1=0.7 bar (table 7).

At u_2>0.8625 the value of Φ_2 did not change, so we considered it as the upper limit of the valve V_2. At lower values of u_2 the value of Φ_2 could not be obtained, because the used flow-meter can not measure flows below 0.03 l/s (see [1]).

The procedure to obtain a valve model was similar to the one presented above with the exception that Δp in expression (1) changes (see Fig. 2):

$$\Phi_2 = K_2 \sqrt{p_1 + K_W \left(h_1 - h_{R2} \right)} \ , \tag{6}$$

where constant K_W=0.0981 bar/m represents the proportional factor between water level in meters and pressure in bars and constant h_{R2}=2 m represents the height of the reservoir R_2 (see Fig. 2).

u_2 [-]	Φ_2 [l/s]	h_1 [m]
0.85	0.308	1.434
0.8	0.254	1.420
0.75	0.202	1.415
0.7	0.160	1.415
0.65	0.131	1.416
0.6	0.106	1.421
0.55	0.083	1.427
0.5	0.073	1.434
0.45	0.053	1.443

Table 7: Measurements on the second valve

From (6), constant K_2 was expressed at different values of u_2 (Table 8).

u_2 [-]	$K_2 \left[\frac{l}{s\sqrt{bar}} \right]$
0.85	0.384
0.8	0.317
0.75	0.252
0.7	0.2
0.65	0.164
0.6	0.132
0.55	0.104
0.5	0.091
0.45	0.066

Table 8: Characteristics of the second valve

With the similar procedure as for the first valve, we derived the model of the second valve:

$$K_2 = K_{02} \cdot R_2^{\,v_2 - 1} = 0.742 \cdot 75.66^{v_2 - 1} \left[\frac{l}{s\sqrt{bar}} \right] \tag{7}$$

Fig. 5 shows the difference between measurements (marked with asterisk) and the estimated function (7).

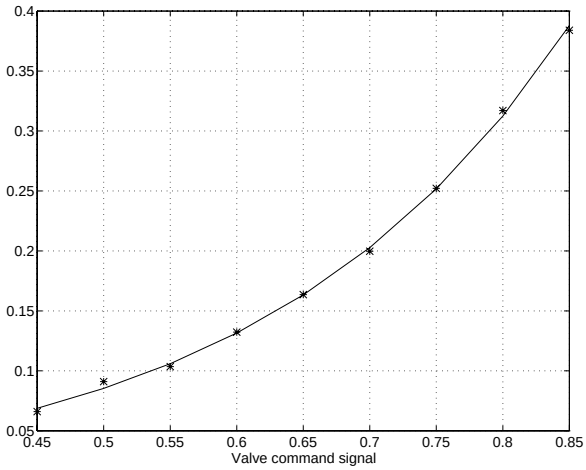

*Fig. 5. Characteristics of the valve V_2 - flow coefficient K_2 vs. valve command signal v_2; * measurements, __ model*

The entire model of V_2 is similar to that of V_1. The only difference is that in the model of V_2 we have to add a range limiter because v_2 saturates at the value u_2=0.8625:

$$v_2 = \begin{cases} u_{2\max} & if\ u_2 > u_{2\max} \\ 0 & if\ u_2 < 0 \\ u_2 & otherwise \end{cases} \tag{8}$$

where

$$u_{2_{\max}} = 0.8625 \tag{9}$$

Hence the entire valve model of the valve V_2 is as shown in Figure 6.

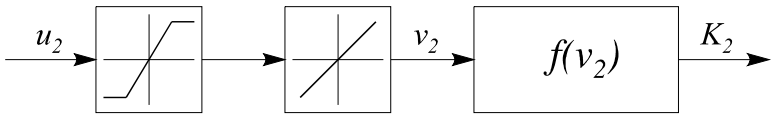

Fig. 6. The entire valve model

2.2 Water and air flow through injector

Both flow (Φ_w) and gas flow (Φ_{air}) are not measured, therefore they were calculated from flows Φ_1 and Φ_2 and the change of water level (dh_1/dt), by the following equations

$$\Phi_w = \Phi_2 + \frac{S_1}{K_F}\frac{dh_1}{dt} \tag{10}$$

$$\Phi_{air} = \Phi_1 - \frac{p_0 + p_1}{p_0}\frac{S_1}{K_F}\frac{dh_1}{dt}\bigg|_{p_1=const.} \tag{11}$$

where constant K_F=0.001 m^3/l represents the proportional factor between m^3/s and l/s. Flows are expressed in [l/s], p_1 in [bar] and h_1 in [m]. S_1 represents the surface of the separator R_1 and is measured as S_1=0.312 m^2. Table 9 gives the obtained measurements.

p_1 [bar]	Φ_1 [l/s]	Φ_2 [l/s]	$\frac{dh_1}{dt}\left[\frac{m}{s}\right]$
0.3	5.85	0.173	$-3\cdot10^{-5}$
0.4	5.91	0.170	$-4\cdot10^{-6}$
0.5	5.70	0.175	$-3.5\cdot10^{-5}$
0.6	5.51	0.175	$-5\cdot10^{-5}$
0.7	5.23	0.174	$-2.5\cdot10^{-5}$

Table 9: Measurements at different pressure p_1

From (7), (8) and table 9, we obtained water and gas flows at different pressures p_1 as written in table 10.

p_1 [bar]	Φ_w [l/s]	Φ_{air} [l/s]
0.3	0.164	5.838
0.4	0.169	5.908
0.5	0.164	5.684
0.6	0.159	5.485
0.7	0.166	5.217

Table 10: Water and air flows vs. pressure p_1

From table 10 it can be seen that water flow does practically not depend on the pressure p_1 and stays more or less unchanged. Therefore, it was modelled as a constant value. The mean value from the values in table 10 is taken:

$$\Phi_w = 0.1644 \left[\frac{l}{s}\right] \tag{12}$$

Air flow depends on pressure p_1 (see table 10). Because changes from p_1=0.3 bar to p_1=0.7 bar cause only about 10% change in Φ_{air}, we modelled it with a linear function:

$$\Phi_{air} = \Phi_{air0} + \Phi_{air1} \cdot p_1 = 6.46 - 1.615 \cdot p_1 \left[\frac{l}{s}\right] \tag{13}$$

Measurements (marked with asterisk) and compared model (13) are shown in Fig. 7.

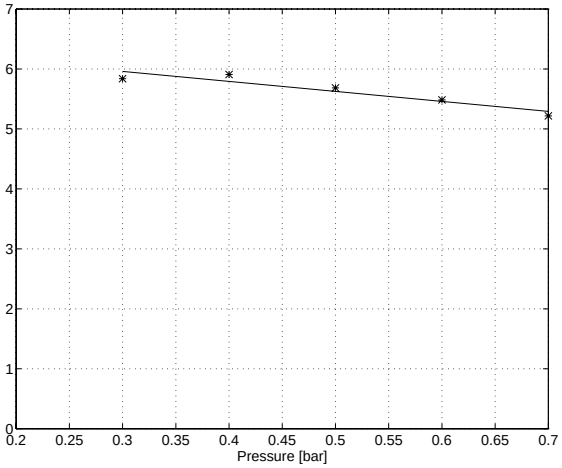

*Fig. 7. Air flow [l/s]; * Measurements, __ Model*

2.3 Air pressure in the separator

To obtain the differential equation for air pressure in the separator, we used the following equation for the isothermal gas change (see Fig. 8):

$$\frac{pV}{m} = rT = const.\ , \tag{14}$$

where p, V and m are absolute air pressure (p_0+p_1), gas volume and mass of the air inside R_1, respectively.

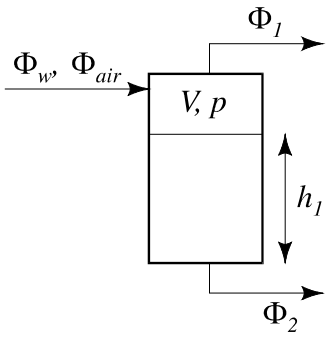

Fig. 8. Flows in the separation unit

The time derivation of the equation (14) is equal to 0, which leads to the next expression:

$$mV\frac{dp}{dt} = pV\frac{dm}{dt} - mp\frac{dV}{dt} \tag{15}$$

The mass of air *m* is:

$$m = \rho V \tag{16}$$

where ρ is air density. The time derivation of the gas mass is proportional to the difference between the input and output air flows:

$$\frac{dm}{dt} = \rho_0\left(\Phi_{air} - \Phi_1\right)K_F \tag{17}$$

where ρ_0 denotes the normal atmospheric air density.

Substituting (17) for d*m*/dt and (16) for *m* in (15), the d*p*/dt can be written

$$\frac{dp}{dt} = \frac{p\rho_0}{\rho V}\left(\Phi_{air} - \Phi_1\right)K_F + \frac{pS_1}{V}\frac{dh_1}{dt} \tag{18}$$

Taking into account that $p/p_0=\rho/\rho_0$ and that $p=p_0+p_1$ leads us to the following expression:

$$\frac{dp_1}{dt} = \frac{1}{V}\left[p_0\left(\Phi_{air} - \Phi_1\right)K_F + \left(p_0 + p_1\right)S_1\frac{dh_1}{dt}\right] \tag{19}$$

where *V* denotes the volume of gas inside the separator R_1 which equals to (see Fig. 2):

$$V = S_1\left(h_{R1} - h_1\right) = S_1\left(2.25 - h_1\right) \tag{20}$$

where h_{R1} denotes the height of the separator R_1 (see Fig. 2).

2.4 Water levels in the separator and reservoir

To obtain a complete model of the separator, we used the following differential equations:

$$\frac{dh_1}{dt} = \frac{1}{S_1}\left(\Phi_w - \Phi_2\right)K_F \tag{21}$$

$$\frac{dh_2}{dt} = \frac{1}{S_2}\left(\Phi_2 - \Phi_w\right)K_F \tag{22}$$

where constant K_F=0.001 m^3/l denotes the factor between units m^3/s and l/s.

2.5 Summary of the non-linear dynamic model

The complete process model can be described by the following expressions:

Valve V_1:
$$K_1 = K_{01} \cdot R_1^{\,v_1 - 1} = 75.1 * 46.1^{v_1 - 1} \tag{23}$$

$$v_1 = \begin{cases} 1 & if\ u_2 > 1 \\ 0 & if\ u_2 < 0 \\ u_1 & otherwise \end{cases} \tag{24}$$

Valve V_2:
$$K_2 = K_{02} \cdot R_2^{\,v_2 - 1} = 0.742 * 75.66^{v_2 - 1} \tag{25}$$

$$v_2 = \begin{cases} u_{2\max} & if\ u_2 > u_{2\max} \\ 0 & if\ u_2 < 0 \\ u_2 & otherwise \end{cases} \tag{26}$$

$$u_{2_{\max}} = 0.8625 \tag{27}$$

The speed limit of valves positions:

$$\dot{v} = \begin{cases} \dot{v}_{\max} & if\ \dot{u} > \dot{v}_{\max} \\ \dot{v}_{\min} & if\ \dot{u} < \dot{v}_{\min} \\ \dot{u} & otherwise \end{cases} \tag{28}$$

$$\dot{v}_{\max} = 0.66 s^{-1} \tag{29}$$

$$\dot{v}_{\min} = -0.33 s^{-1} \tag{30}$$

Air flow through valve V_1: $$\Phi_1 = K_1 \sqrt{p_1} \ \text{[l/s]}, \tag{31}$$

Water flow through valve V_2:

$$\Phi_2 = K_2 \sqrt{p_1 + K_W \left(h_1 - h_{R2} \right)} \ \text{[l/s]}, \tag{32}$$

Water flow to the separator R_1: $$\Phi_w = 0.1644 \ \text{[l/s]} \tag{33}$$

Air flow to the separator R_1:

$$\Phi_{air} = \Phi_{air0} + \Phi_{air1} \cdot p_1 = 6.46 - 1.615 \cdot p_1 \ \text{[l/s]} \tag{34}$$

Change of water level in R_1:

$$\frac{dh_1}{dt} = \frac{1}{S_1} \left(\Phi_w - \Phi_2 \right) K_F \ \text{[m/s]} \tag{35}$$

Change of water level in R_2:

$$\frac{dh_2}{dt} = \frac{1}{S_2} \left(\Phi_2 - \Phi_w \right) K_F \ \text{[m/s]} \tag{36}$$

Change of air pressure inside R_1:

$$\frac{dp_1}{dt} = \frac{1}{V} \left[p_0 \left(\Phi_{air} - \Phi_1 \right) K_F + \left(p_0 + p_1 \right) \left(\Phi_w - \Phi_2 \right) K_F \right] \ \text{[bar/s]} \tag{37}$$

Air volume inside R_1:

$$V = S_1\left(h_{R1} - h_1\right) = S_1\left(2.25 - h_1\right) \ [\mathrm{m}^3] \tag{38}$$

Cross-section of R_1: $$S_1 = 0.312m^2 \tag{39}$$

Cross-section of R_2: $$S_2 = 0.32m^2 \tag{40}$$

Mathematical model of the gas-liquid separator was simulated in MATLAB-SIMULINK environment. The simulation scheme is shown in Fig. 9.

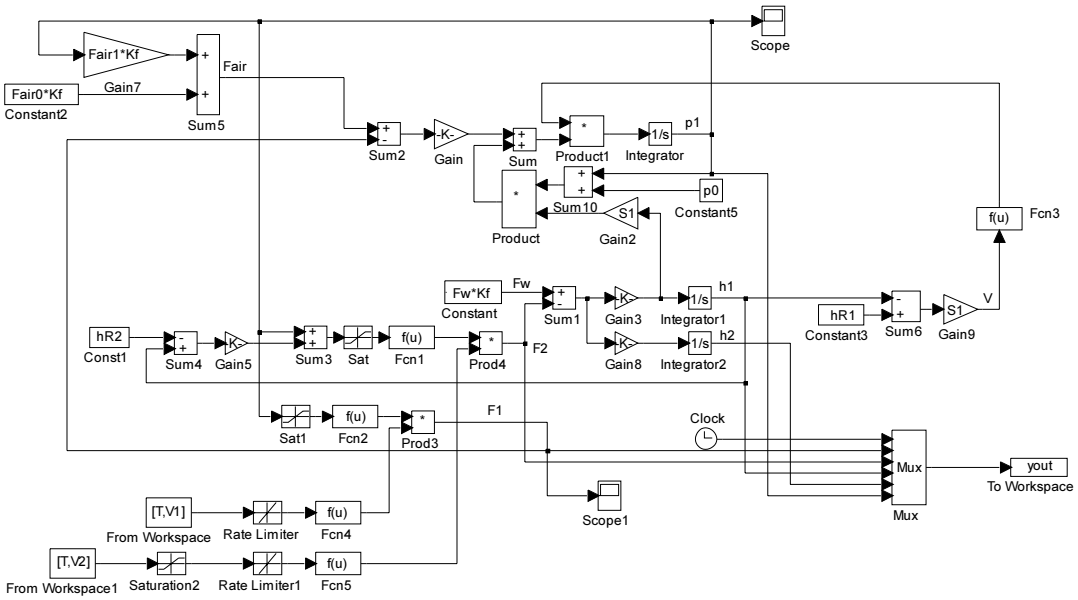

Fig. 9. Simulation scheme of the liquid-gas separator in program package SIMULINK

2.6 Steady-state analysis

The process has a limited steady-state working range. The maximum water level in R_1 is limited with the whole water volume in the system to approximately h_{1max}=1.9 m. The minimum water level is limited to h_{1min}=0.9 m, because at lower levels of h_1 water comes out of the reservoir R_2.

The maximum air pressure in R_1 is limited to p_{1max}=1 bar (the range of the pressure transmitter) and the minimum pressure is limited by the water flows Φ_2 and Φ_w. In the steady-state, both flows are the same. So, if gas pressure in R_1 were too small, then Φ_w would be always bigger than Φ_2 even when the valve V_2 were fully opened (u_{2max}=0.8625).

Using equations (25), (32) and (33) we can calculate the minimal p_1 at different water levels h_1 as

$$p_{1\min} = \frac{\Phi_w^{\,2}}{K_{02}^{\,2} R_2^{\,2(0.8625-1)}} - K_w\left(h_1 - h_{R2}\right) \tag{41}$$

The area of the steady state values of p_1 and h_1 is presented in Fig. 10 with a net.

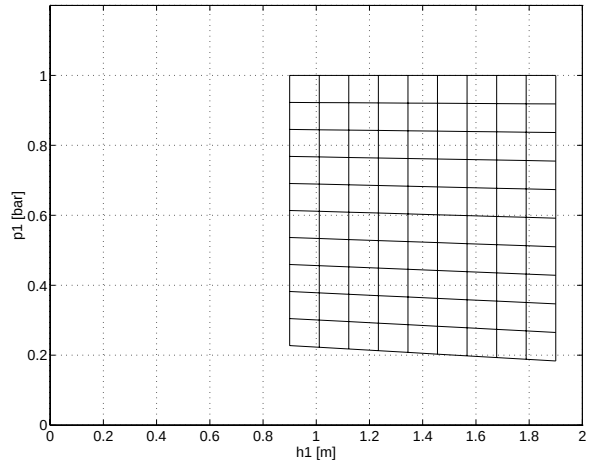

Fig. 10. The steady-state area of values p_1 and h_1

From this area of values p_1 and h_1 we calculated the correspondent steady-state values of v_1 and v_2 (position of the valves V_1 and V_2).

In equations (35) and (37) we set the time derivatives equal to 0 and obtained the steady-state area of values of v_1 and v_2, as shown in Fig. 11.

From Fig. 11 it can be seen that the steady-state area of values v_1 and v_2 is extremely narrow. The consequence is that a small error in the model can lead to a quite large error in the steady-state values of h_1, which can easily exceed the permitted working range. Just a slight deviation from the steady-state values of v_1 and v_2 will cause the model to exceed the working range. Apparently, the plant behaves as if it were an integral process.

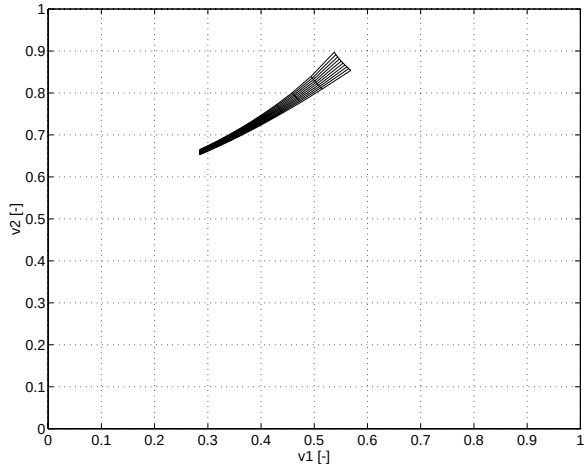

Fig. 11. The steady-state area of values v_1 and v_2

2.7 Linearised dynamic model

From the existing nonlinear model we also obtained a linearised simulation model. The set-point is the steady-state pressure in the separator R_1 (p_{1s}) and the steady-state water level inside the separator (h_{1s}). By changing the valve command signals from the steady-state positions (changes are Δv_1 and Δv_2), we obtained linearised simulation model of the process:

$$\begin{bmatrix} \Delta\dot{p}_1 \\ \Delta\dot{h}_1 \end{bmatrix} = \underline{\underline{A}} \begin{bmatrix} \Delta p_1 \\ \Delta h_1 \end{bmatrix} + \underline{\underline{B}} \begin{bmatrix} \Delta v_1 \\ \Delta v_2 \end{bmatrix} \tag{42}$$

$$\begin{bmatrix} \Delta p_1 \\ \Delta h_1 \\ \Delta\Phi_1 \\ \Delta\Phi_2 \end{bmatrix} = \underline{\underline{C}} \begin{bmatrix} \Delta p_1 \\ \Delta h_1 \end{bmatrix} + \underline{\underline{D}} \begin{bmatrix} \Delta v_1 \\ \Delta v_2 \end{bmatrix} \tag{43}$$

where Δp_1, Δh_1, $\Delta\Phi_1$ and $\Delta\Phi_1$ denote the change of p_1, h_1, Φ_1 and Φ_2 from the steady-state values:

$$\begin{aligned} \Delta p_1 &= p_1 - p_{1s} \\ \Delta h_1 &= h_1 - h_{1s} \end{aligned} \tag{44}$$

The elements of matrices $\underline{A}$ and $\underline{B}$ are the following:

$$
\begin{aligned}
a_{11} &= \frac{K_F}{V_{1s}}\left[p_0\left(\Phi_{air1} - \frac{K_{1s}}{2\sqrt{p_{1s}}} \right) - \left(p_0 + p_{1s} \right) \frac{K_{2s}}{2\sqrt{p_{V2s}}} \right] \\
a_{12} &= -\frac{K_F}{V_{1s}}\left[\left(p_0 + p_{1s} \right) \frac{K_{2s} K_w}{2\sqrt{p_{V2s}}} \right] \\
a_{21} &= -\frac{K_F}{S_1}\left[\frac{K_{2s}}{2\sqrt{p_{V2s}}} \right] \\
a_{22} &= -\frac{K_F}{S_1}\left[\frac{K_{2s} K_w}{2\sqrt{p_{V2s}}} \right]
\end{aligned}
\tag{45}
$$

$$
\begin{aligned}
b_{11} &= -\frac{K_F}{V_{1s}} p_0 K_{1s} \sqrt{p_{1s}} \ln\left(R_1 \right) \\
b_{12} &= -\frac{K_F}{V_{1s}} \left(p_0 + p_{1s} \right) K_{2s} \sqrt{p_{V2s}} \ln\left(R_2 \right) \\
b_{21} &= 0 \\
b_{22} &= -\frac{K_F}{S_1} K_{2s} \sqrt{p_{V2s}} \ln\left(R_2 \right)
\end{aligned}
\tag{46}
$$

$$
\begin{aligned}
c_{11} &= 1 \\
c_{12} &= 0 \\
c_{21} &= 0 \\
c_{22} &= 1 \\
c_{31} &= \frac{K_{1s}}{2\sqrt{p_{1s}}} \\
c_{32} &= 0 \\
c_{41} &= \frac{K_{2s}}{2\sqrt{p_{V2s}}} \\
c_{42} &= \frac{K_{2s} K_w}{2\sqrt{p_{V2s}}}
\end{aligned}
\tag{47}
$$

$$
\begin{aligned}
d_{11} &= K_{1s} \sqrt{p_{1s}} \ln\left(R_1 \right) \\
d_{12} &= 0 \\
d_{21} &= 0 \\
d_{22} &= K_{2s} \sqrt{p_{V2s}} \ln\left(R_2 \right)
\end{aligned}
\tag{48}
$$

where K_{1s}, K_{2s} and V_{1s} denote the steady-state values of K_1, K_2 and V, respectively. The steady-state pressure on the valve V_2 is marked as p_{V2s} and is equal to

$$p_{V2s} = p_1 + K_w\left(h_1 - h_{R2}\right) \tag{49}$$

The linearised simulation scheme in program package SIMULINK is shown in Fig. 12.

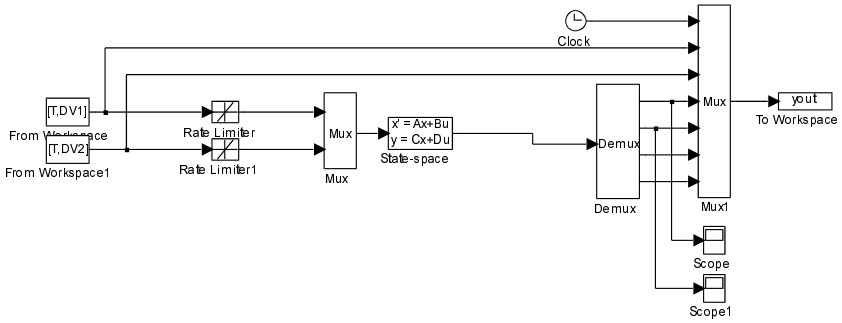

Fig. 12. The linearised simulation scheme in program package SIMULINK

3. Cross-validation of the dynamic model

3.1 Cross-validation of the nonlinear dynamic model

Verification of the obtained model was performed by the open-loop and closed-loop measurements. First we changed the positions of the valves V_1 and V_2 manually. Figure 13 shows the signals on both valves.

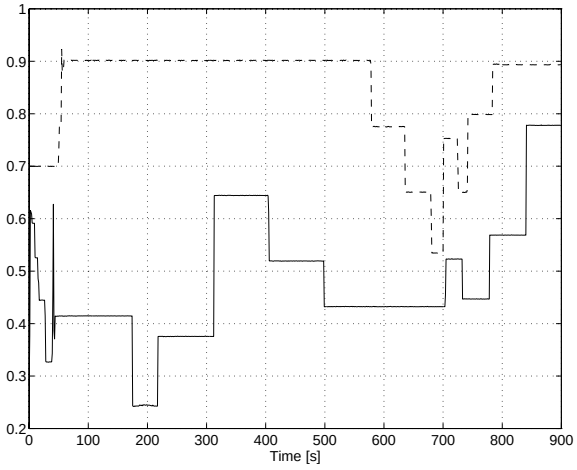

Fig. 13. Valve command signals; __ v_1, -- v_2

Figures 14 to 17 show the measurements (dashed lines) and the results obtained by the mathematical model (full lines). Fig. 14 shows the response of gas pressure (p_1) in the separator. The liquid level h_1 is shown in Fig. 15. We can see the difference between measurements and model because of its apparently integral character. Figures 16 and 17 show the flow through both valves (V_1 and V_2). As it can be seen, the results of the model are quite good (in this case even for the water level h_1).

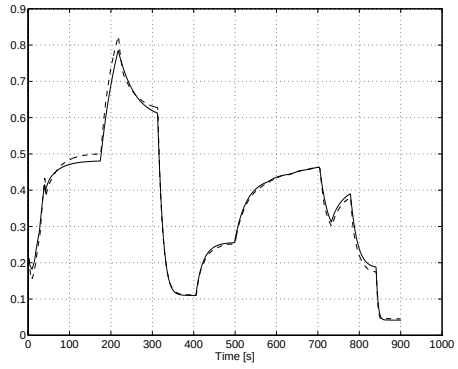

Fig. 14. Gas pressure in the separator (p_1) in [bar]; __ model, -- measurements

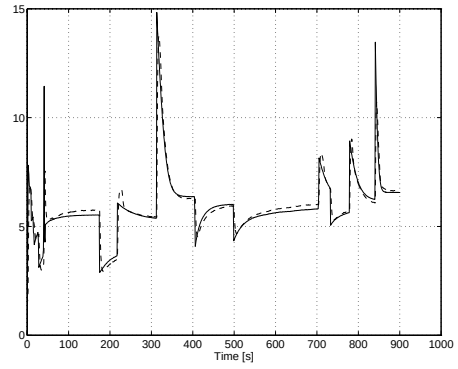

Fig. 16. Air flow Φ_1 through the valve V_1 in [l/s]; __ model, -- measurements

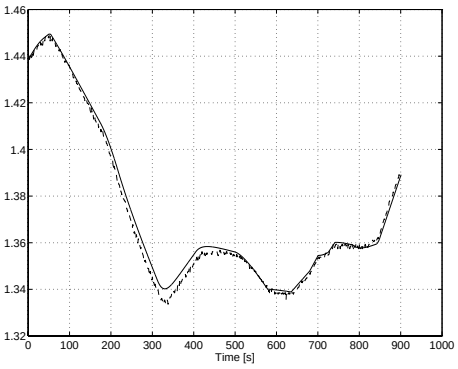

Fig. 15. Liquid level in the separator (h_1) in [m]; __ model, -- measurements

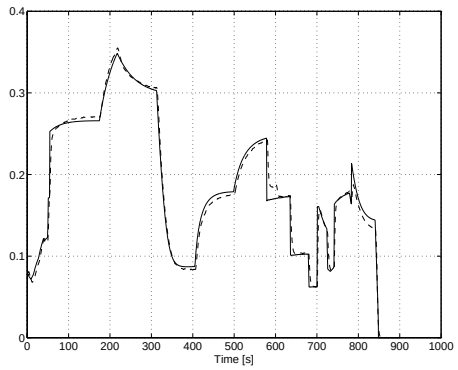

Fig. 17. Liquid flow Φ_2 through the valve V_2 in [l/s]; __ model, -- measurements

The closed-loop experiment was also performed to verify the mathematical model. Two digital PI controllers were used. The first controlled gas pressure in the separator R_1 by changing the position of the valve V_1 and the second one was used to control the liquid level in the separator by changing the position of the valve V_2.

The scheme of the controller is shown in Fig. 18.

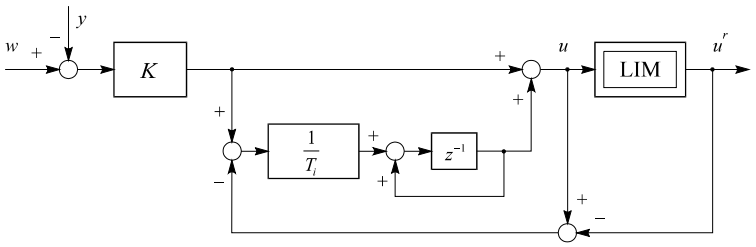

Fig. 18. The scheme of a discrete PI controller

Here LIM represents the controller limitations (from 0 to 1), w is the reference (pressure or level), y is the measured value (actual pressure or level) and u^r is the output of the controller (signal to the valves - u_1 or u_2). The inner closed-loop from limitations to the integrator input represents the anti-windup compensator (for more details see [3]). The sampling time was 1s and the controller parameters were:

$$\begin{aligned} K_1 &= -2; \quad T_{i1} = 10 \\ K_2 &= -10; \quad T_{i2} = 1000 \end{aligned} \tag{50}$$

where indexes 1 and 2 denote pressure and level controller parameters, respectively. Fig. 19 shows the closed-loop control realised in a program package SIMULINK.

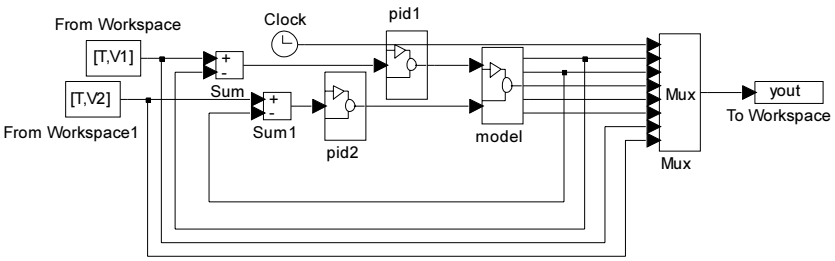

Fig. 19. The closed-loop realisation in SIMULINK

Fig. 20 shows the applied reference signals for gas pressure (p_1) and liquid level (h_1).

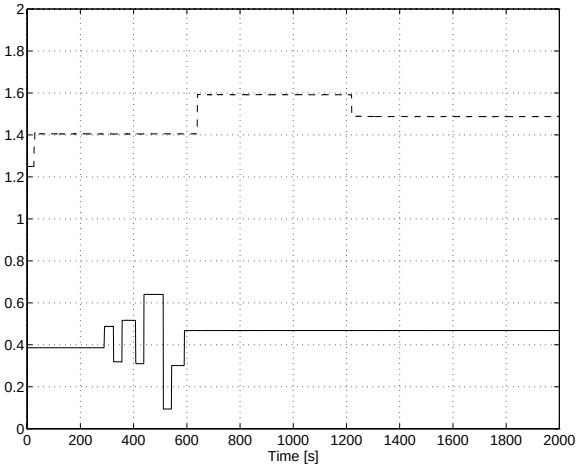

Fig. 20. References; __ gas pressure [bar]; -- liquid level [m]

The closed-loop experiment was made and the model verification is provided in the open-loop (inputs to the process model are the output values of PI controllers). The results are shown in Figures 21 to 24. We can see quite a big difference in water level inside R_1 between the model and real system because the level is quite sensitive even to very small differences in modelled flows Φ_w and Φ_2 compared to real (measured) ones.

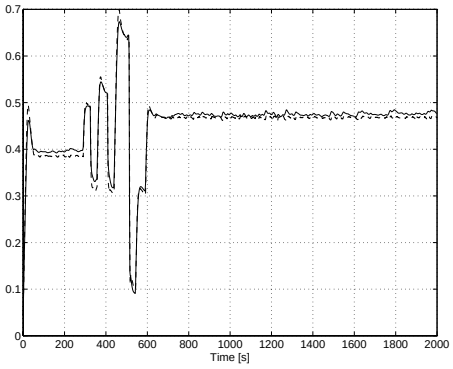

Fig. 21. Gas pressure in the separator (p_1) in [bar]; __ model, -- measurements

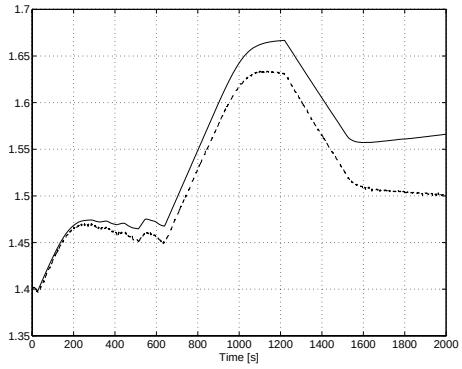

Fig. 22. Liquid level in the separator (h_1) in [m]; __ model, -- measurements

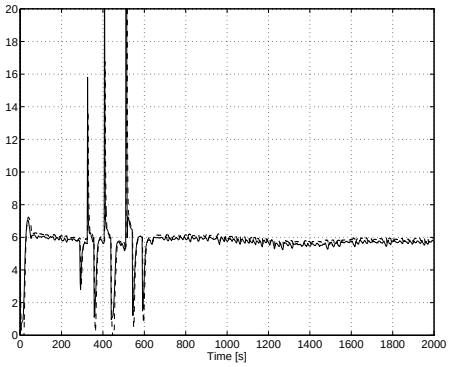

Fig. 23. Air flow Φ_1 through the valve V_1 in [l/s]; __ model, -- measurements

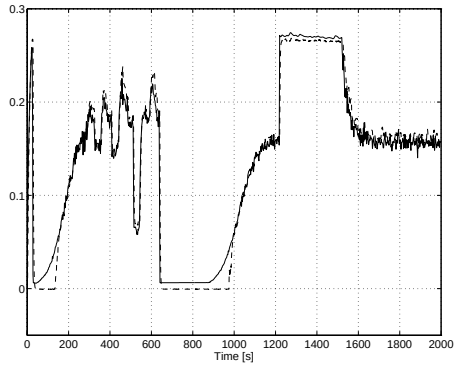

Fig. 24. Liquid flow Φ_2 through the valve V_2 in [l/s]; __ model, -- measurements

The results of the simulated closed-loop system (see Fig. 19) are shown in Figures 25 to 30.

Figures 25 and 26 show the gas pressure and liquid level in the separator. The difference between measurements and model are quite small.

Flows through the valves V_1 and V_2 are shown in Figures 27 and 28. We can see that differences between measurements and model exist at lower flows. The reason lies in the fact that flow-meters can not measure flows below 1.5 l/s for gas and below 0.03 l/s for fluid (water) flow (see [1]), as can be easily seen from measurements.

Figures 29 and 30 show the controllers outputs (limited).

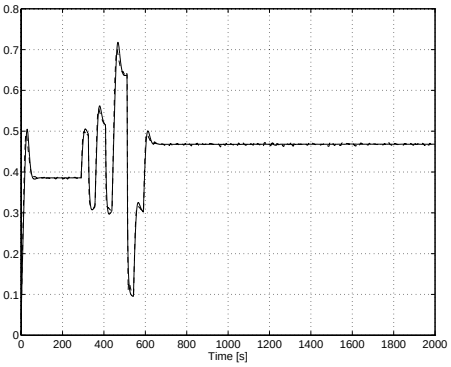

Fig. 25. Gas pressure in the separator (p_1) in [bar]; __ model, -- measurements

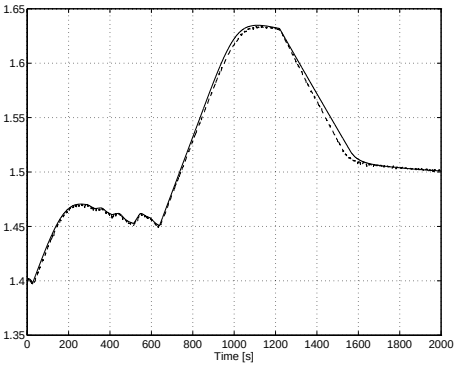

Fig. 26. Liquid level in a separator (h_1) in [m]; __ model, -- measurements

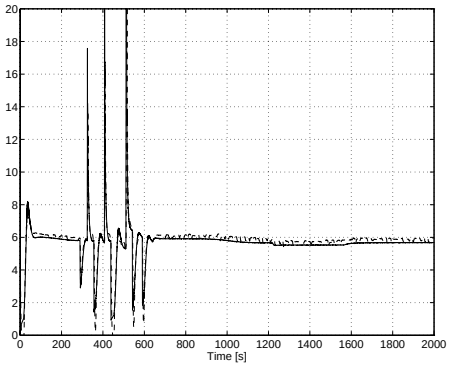

Fig. 27. Gas flow Φ_1 through the valve V_1 in [l/s]; __ model, -- measurements

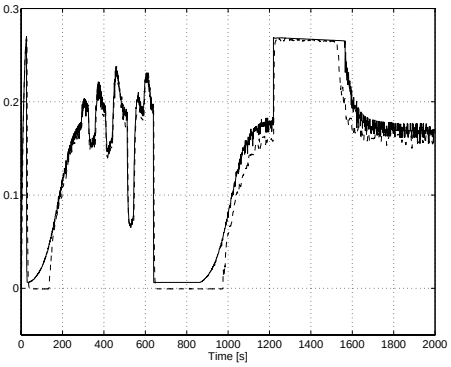

Fig. 28. Liquid flow Φ_2 through the valve V_2 in [l/s]; __ model, -- measurements

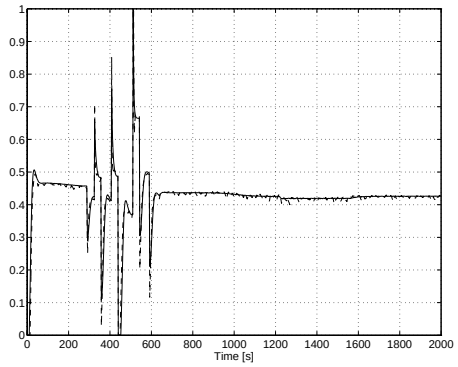

Fig. 29. Limited pressure controller output; __ model, -- measurements

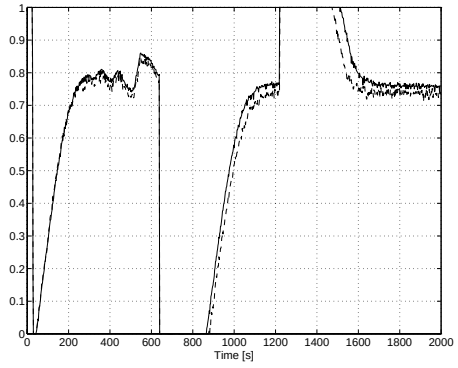

Fig. 30. Limited level controller output; __ model, -- measurements

3.2 Validation of the linearised dynamic model

Validation of the linearised dynamic model is also performed. Fig. 31 shows the input excitation (the change of signals v_1 and v_2 from the steady-state positions). Figures 32 to 35 show the result of the experiment when process is excited around the set-point (p_{1s}=0.5 bar, h_{1s}=1.4 m). It can be seen that the simulated water level, as in the non-linear open-loop experiment, has a drift when compared to the measured level.

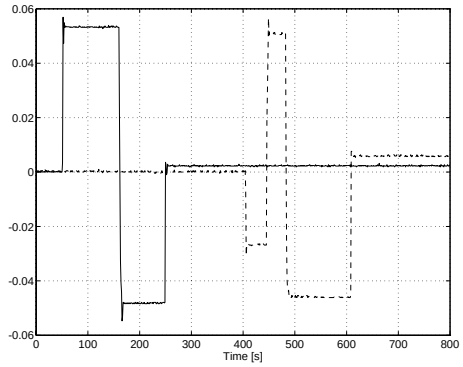

Fig. 31. Input excitation (deviation from the steady-state positions);
__ Δu_1 [-]; -- Δu_2 [-];

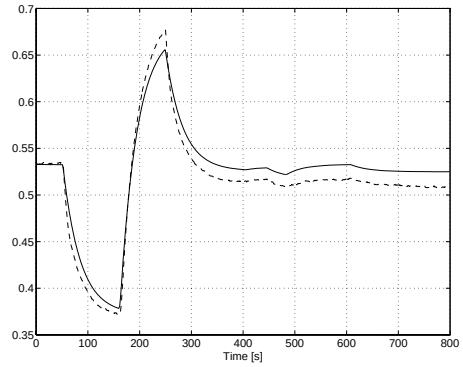

Fig. 32. Gas pressure in the separator (p_1) in [bar]; __ model, -- measurements

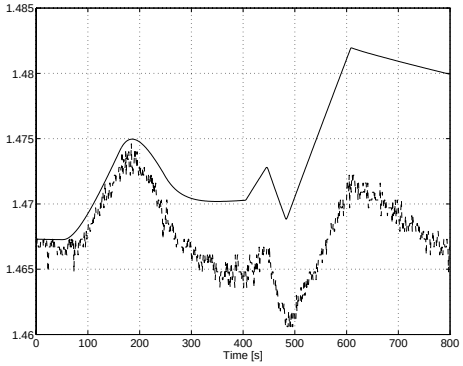

Fig. 33. Liquid level in a separator (h_1) in [m]; __ model, -- measurements

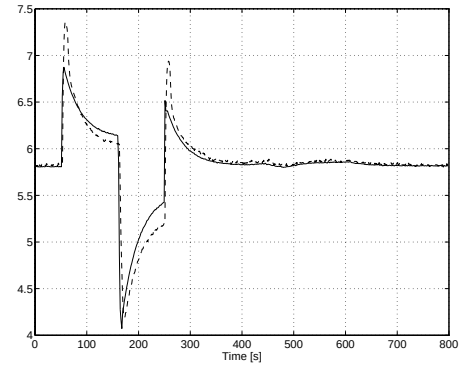

Fig. 34. Gas flow Φ_1 through the valve V_1 in [l/s]; __ model, -- measurements

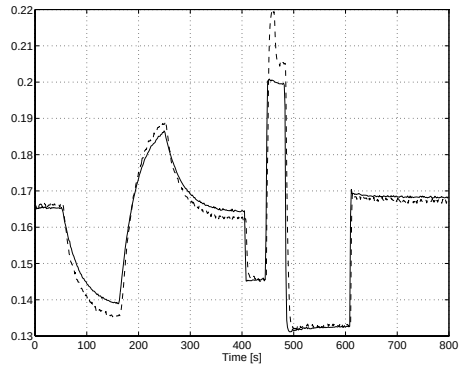

Fig. 35. Liquid flow Φ_2 through the valve V_2 in [l/s]; __ model, -- measurements

4. Faults

Table 11 gives a list of some possible faults.

No.	*Type of fault*	*Realisation*
1	partially clogged injector I_1	built-in
2	leak in R_1	built-in
3	leak in R_2	built-in
4	offset in level transmitter LT_1	emulated
5	fault in flow transmitter FT_1	emulated
6	fault in flow transmitter FT_2	emulated
7	fault in pressure transmitter PT_1	emulated
8	fault in valve V_1 (friction)	emulated
9	fault in valve V_2 (friction)	emulated

Table 11. List of faults

4.1 Component faults: open-loop experiment

We first made open-loop and closed-loop experiments with built-in component faults (see table 11). In these experiments the air flow to the separator R_1 was decreased and leaks in R_1 and R_2 were provoked.

Signals on the valves V_1 and V_2 (v_1 and v_2) during the open-loop experiment are shown in Fig. 36. They were kept constant during the experiment. Fig. 37 shows the modelled and measured pressure (p_1) in the separator R_1. We can see that clogged injector I_1 causes significant drop in gas pressure. The same, but less significant effect can be observed when R_1 is leaking. Fig. 38 shows the water level h_1. Significant change of the measured water level at 300s and 500s can be seen. Both, clogged injector and leak in R_1, cause significant change in h_1. The water level in R_2 (h_2) is shown in Fig. 39. Similarly as for the h_1, significant change in level h_2 caused by the clogged injector and leak in R_2 can be observed. Leaks in R_1 and R_2 can be observed easier when comparing model and measurements of the sum of h_1 and h_2. Fig. 40 shows the sum of water volumes in R_1 and R_2. When leaks in R_1 and R_2 occurred, significant changes between measurements and model can be observed. Figures 41 and 42 show flows through the valves V_1 and V_2 (Φ_1 and Φ_2). respectively. It can be seen that both flows are particularly sensitive to the clogged injector.

Fault	*Time of fault*	*Duration of fault*
Partially clogged injector I_1	300s	30s
Leak in R_1 (valve V_3 opened)	500s	30s
Leak in R_2	700s	30s

Table 12. Realised faults during experiments

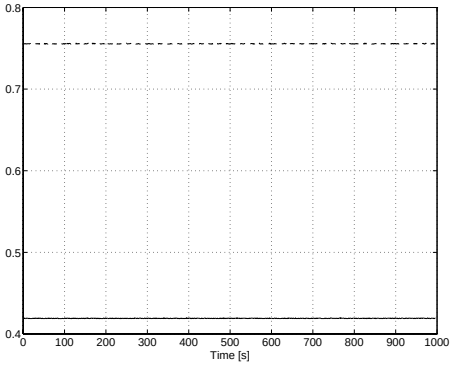

Fig. 36. Valves command signals v_1 and v_2 during the open-loop experiment; __ v_1, -- v_2

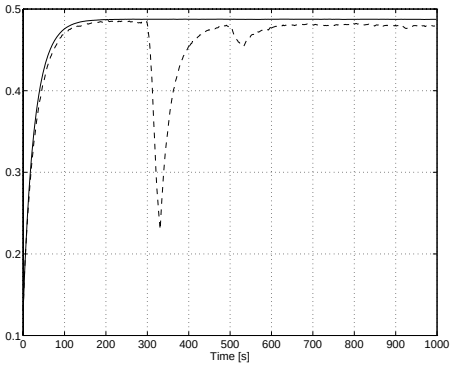

Fig. 37. Pressure in the separator (p_1) in [bar]; __ model; -- measurements

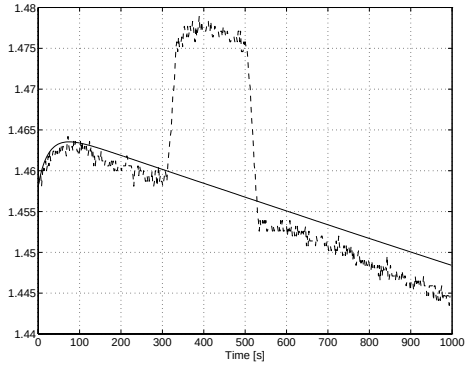

Fig. 38. Water level h_1 in R_1 in [m]; __ model; -- measurements

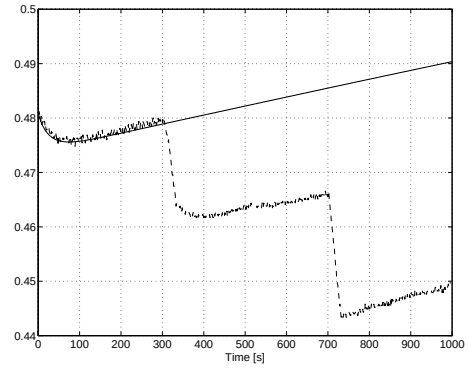

Fig. 39. Water level h_2 in R_2 in [m]; __ model; -- measurements

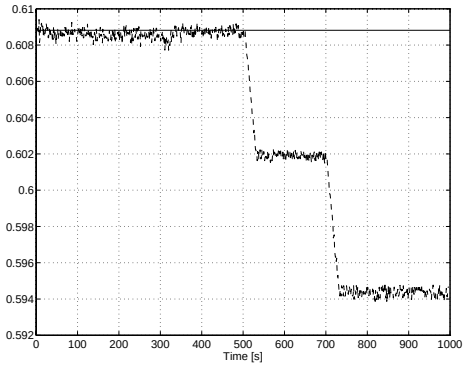

Fig. 40. The sum of water volumes in the separator R_1 and reservoir R_2 in [m^3]; __ model; -- measurements

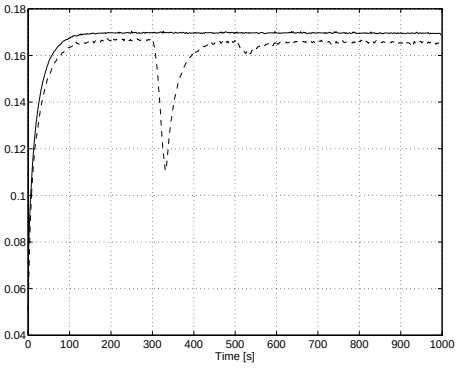

Fig. 42. Water flow Φ_2 through the valve V_2 in [l/s]; __ model, -- measurements

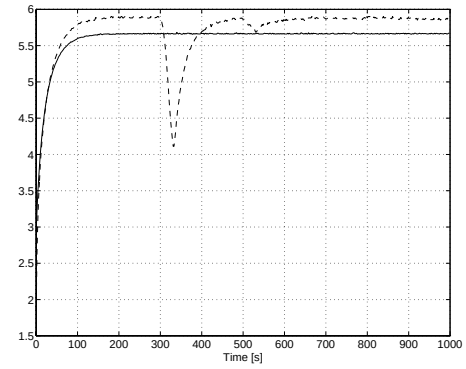

Fig. 41. Air flow Φ_1 through the valve V_1 in [l/s]; __ model, -- measurements

4.2 Component faults: closed-loop experiment

Similarly as in the open loop experiment, we made measurements with the same faults while the system was running in closed-loop. The duration of faults 2 and 3 (leaks in R_1 and R_2) were slightly shorter (about 10 s and 25 s, respectively). We used the same controllers as for the model validation (see expression (16)). References for pressure and level are shown in Fig. 43. Pressure p_1 in the separator is shown in Fig. 44. We can see that PI controller succeeded to keep the pressure p_1 near the set-point (0.5 bar), so the changes are much smaller than those obtained by open-loop measurements. Water level in the separator (h_1) is shown in Fig. 45. Because pressure in the separator was kept more or less constant, the significant change of the level can be seen only when R_1 leaks (at 500 s). Fig. 46 shows the water level in the reservoir (h_2). Significant changes between model and measurements can be observed when R_1 and/or R_2 leaks. The same can be observed in Fig. 47, where the sum of both water volumes is presented. The result is similar to the one obtained

by open-loop experiment, as is expected. Fig. 48 and 49 show flows through the valves V_1 and V_2 (Φ_1 and Φ_2). The difference from the open-loop experiment is that flow Φ_2 is much more sensitive to leak in R_1. This is expected, because the PI controller tries to keep the level h_1 constant and when leak in R_1 occurs, it closes the valve V_2 (decreases the flow Φ_2). The limited pressure controller output and level controller output are shown in Figures 50 and 51.

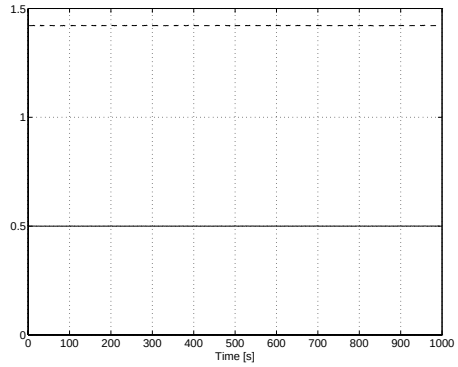

Fig. 43. References for gas pressure and water level in the separator R_1; __ p_1 [bar], -- h_1 [m]

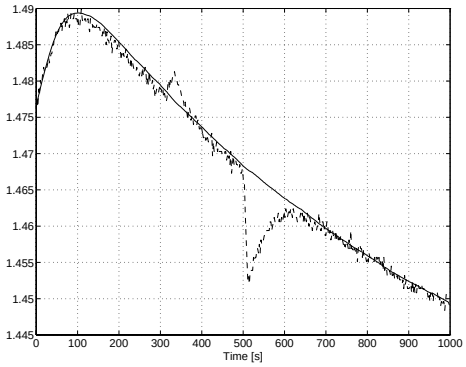

Fig. 45. Water level in the separator R_1 (h_1) in [m]; __ model; -- measurements

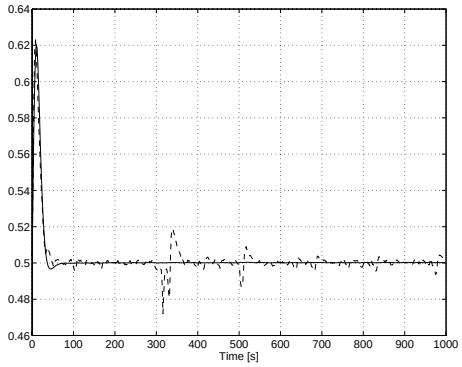

Fig. 44. Pressure in the separator (p_1) in [bar]; __ model; -- measurements

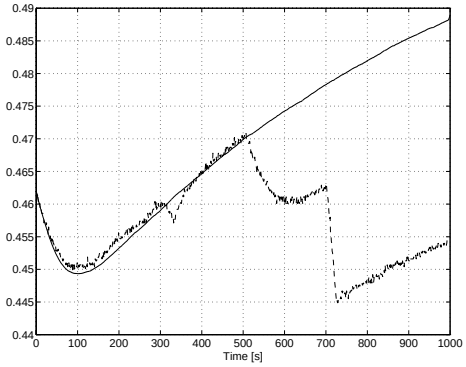

Fig. 46. Water level in the reservoir R_2 (h_2) in [m]; __ model; -- measurements

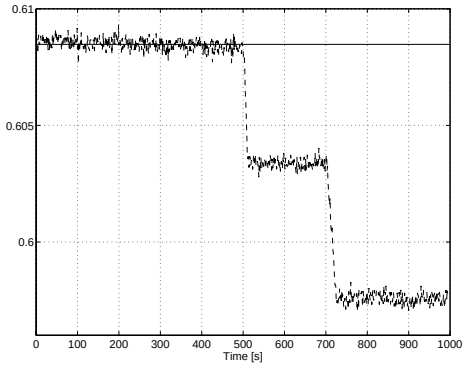

Fig. 47. The sum of water volumes in the separator R_1 and reservoir R_2 in [m^3]; __ model; -- measurements

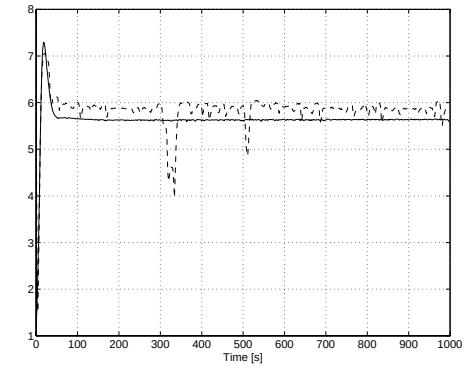

Fig. 48. Air flow Φ_1 through the valve V_1 in [l/s]; __ model, -- measurements

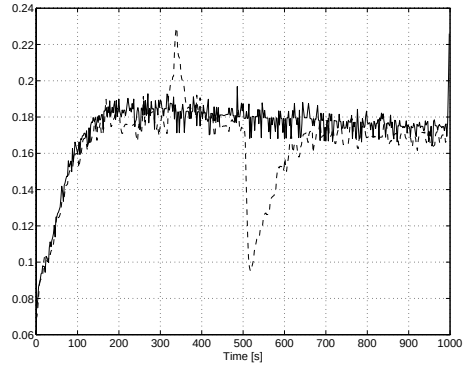

Fig. 49. Water flow Φ_2 through the valve V_2 in [l/s]; __ model, -- measurements

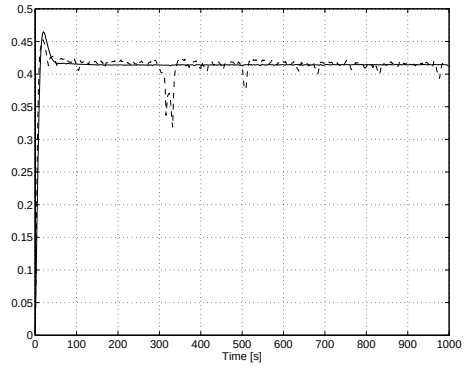

Fig. 50. Limited output of the pressure controller; __ model, -- measurements

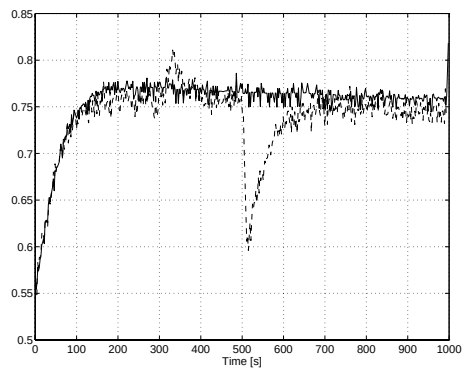

Fig. 51. Limited output of the level controller; __ model, -- measurements

4.3 Transmitters faults: closed-loop experiment

Next measurements were performed with faults in gas pressure transmitter PT_1 and level transmitter LT_1 in the closed-loop configuration. We simulated drift and abrupt change of transmitter values by adding offset signals to transmitter values as shown in Fig. 52.

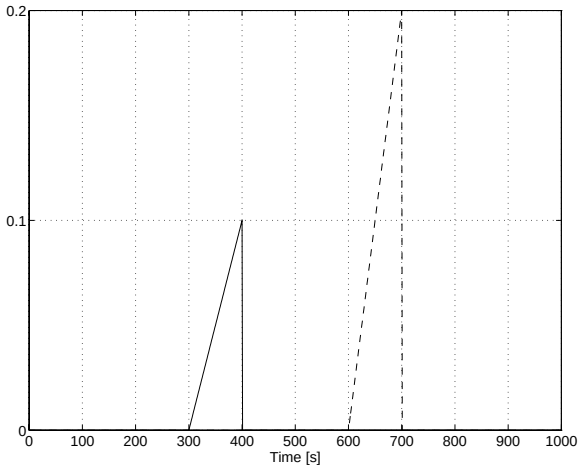

Fig. 52. Offset signals added to the pressure and level transmitters;
__ offset in pressure transmitter PT_1 [bar], -- offset in level transmitter LT_1 [m]

In the experiment, the same controllers are used as for the system validation (see expression (47)). References for pressure p_1 and level h_1 are shown in Fig. 53. Response of pressure p_1 in the separator is shown in Fig. 54 and water level in the separator (h_1) is shown in Fig. 55. Significant change in level can be seen during drift and abrupt change in LT_1. Fig. 56 shows the water level in the reservoir (h_2). As for h_1, significant change in the level h_2 can be observed during drift and abrupt change in LT_1. The same can be observed in Fig. 57, where the sum of both water volumes in R_1 and R_2 is presented. The added fault signal is clearly visible. Fig. 58 and 59 show flows through the valves V_1 and V_2 (Φ_1 and Φ_2). The difference is noticeable during fault in PT_1 for flow Φ_1 and during fault of LT_1 for flow Φ_2. Figures 60 and 61 show the limited controller outputs where the responses are similar to those for Φ_1 and Φ_2.

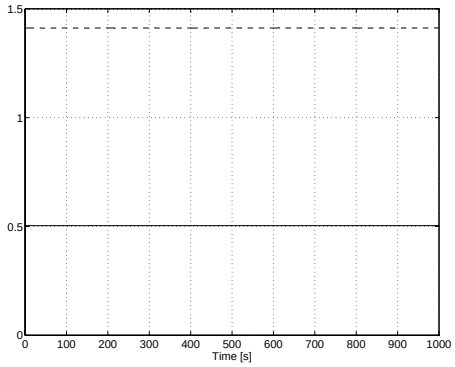

Fig. 53. References for gas pressure and water level in the separator R_1; __ p_1 [bar], -- h_1 [m]

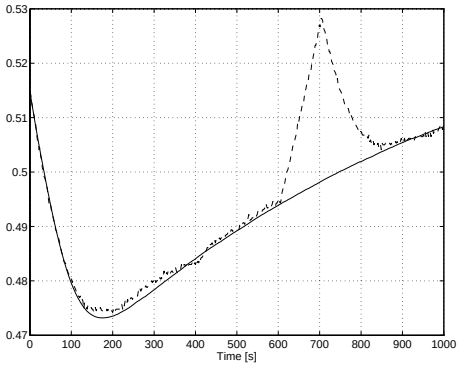

Fig. 56. Water level in the reservoir R_2 (h_2) in [m]; __ model; -- measurements

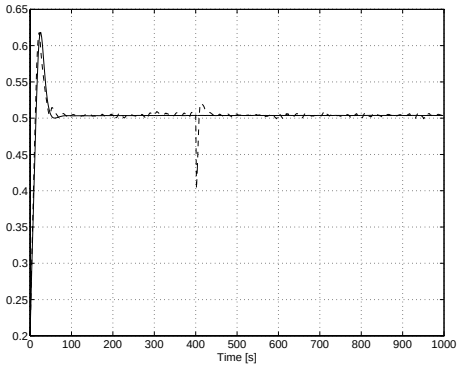

Fig. 54. Pressure in the separator (p_1) in [bar]; __ model; -- measurements

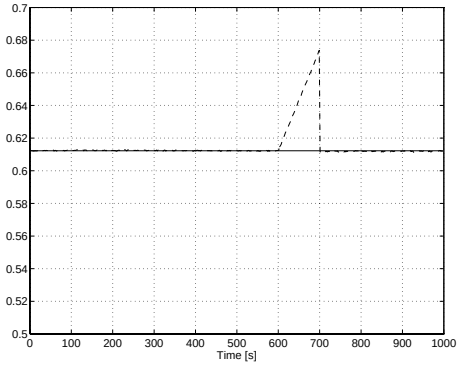

Fig. 57. The sum of water volumes in the separator R_1 and reservoir R_2 in [m^3]; __ model; -- measurements

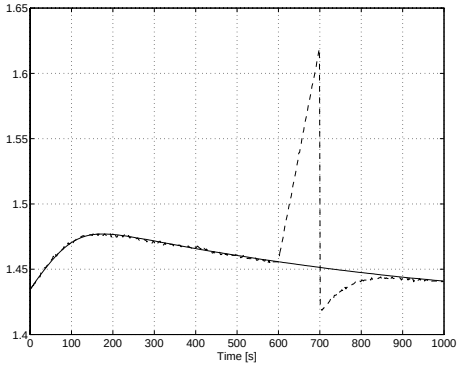

Fig. 55. Water level in the separator R_1 (h_1) in [m]; __ model; -- measurements

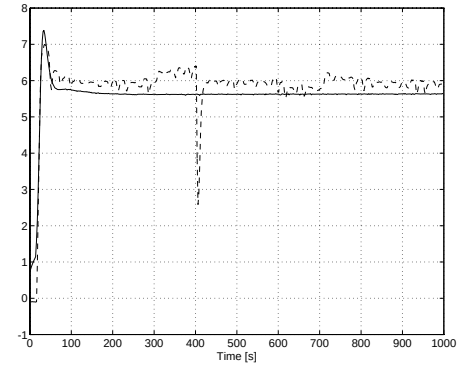

Fig. 58. Air flow Φ_1 through the valve V_1 in [l/s]; __ model, -- measurements

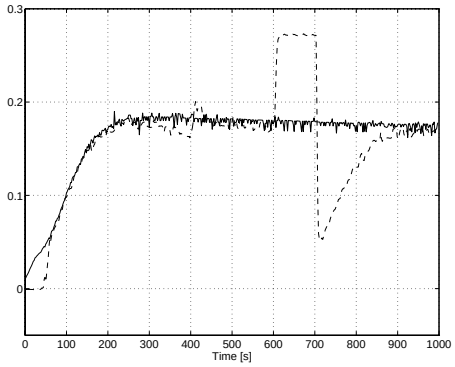

Fig. 59. Water flow Φ_2 through the valve V_2 in [l/s]; __ model, -- measurements

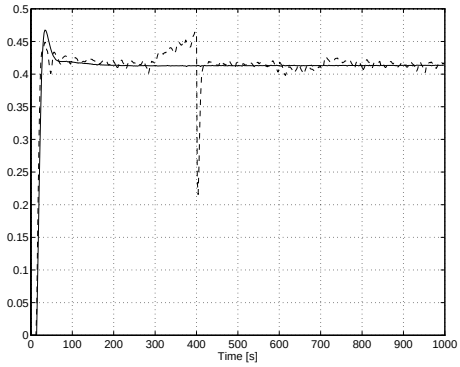

Fig. 61. Limited output of the level controller; __ model, -- measurements

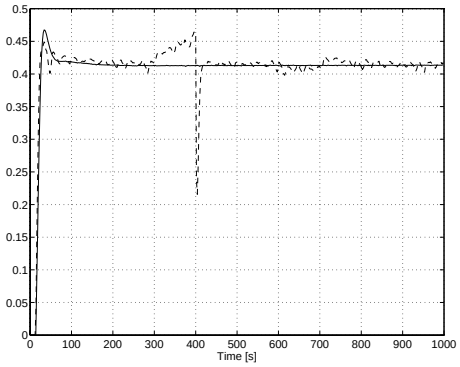

Fig. 60. Limited output of the pressure controller; __ model, -- measurements

4.4 Actuator faults: closed-loop

These measurements were performed on the system so that the actuator faults (on valves V_1 and V_2) were emulated. The offset signals (shown in Fig. 62) are added to the actuator signals.

The same controllers were used as for the system validation (see expression (47)). References for pressure and level were the same as in the previous case. Pressure p_1 in the separator is shown in Fig. 63. Change of the water level in the separator (Fig. 64) can be seen during drift and abrupt change in V_2. Fig. 65 shows water level in the reservoir (h_2). As for h_1, the change of level h_2 can be observed during drift and abrupt change in V_2. Fig. 66 shows the sum of both water volumes in R_1 and R_2. We can see that measurements do not differ from simulations. Fig. 67 and 68 show flows through the valves V_1 and V_2 (Φ_1 and Φ_2). The difference is noticeable during abrupt fault of V_1 for flow Φ_1 and during drift and abrupt fault of V_2 for flow Φ_2. Figures 69 and 70 show the limited controller outputs where one can see the difference during fault on V_1 (for the first controller output) and during and after the fault on V_2 (for the second controller output).

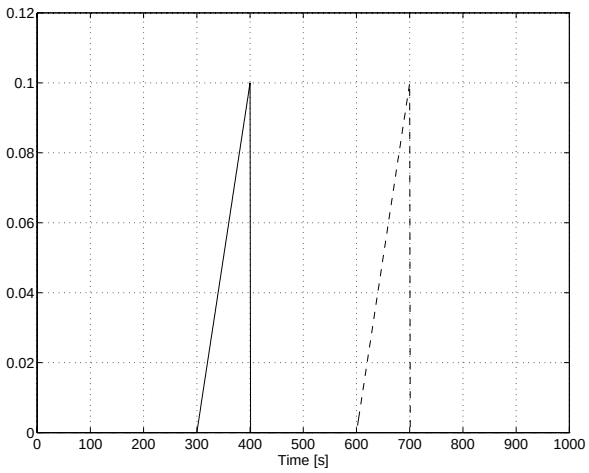

Fig. 62. Offset signals added to the actuators; __ offset in valve V_1 [-], -- offset in valve V_2 [-]

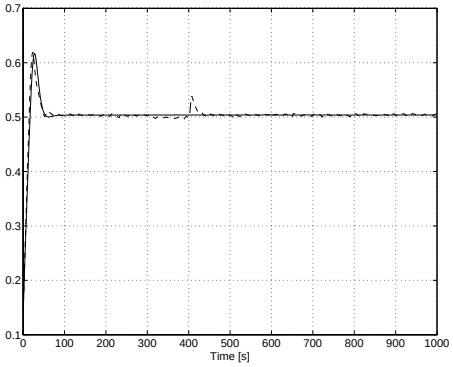

Fig. 63. Pressure in the separator (p_1) in [bar]; __ model; -- measurements

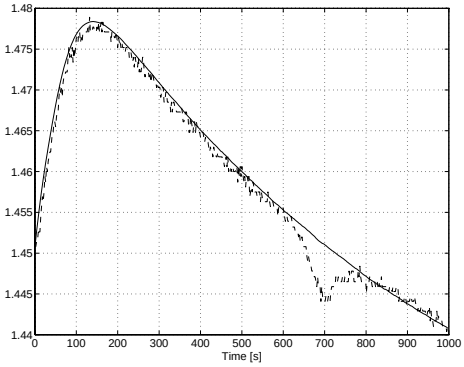

Fig. 64. Water level in the separator R_1 (h_1) in [m]; __ model; -- measurements

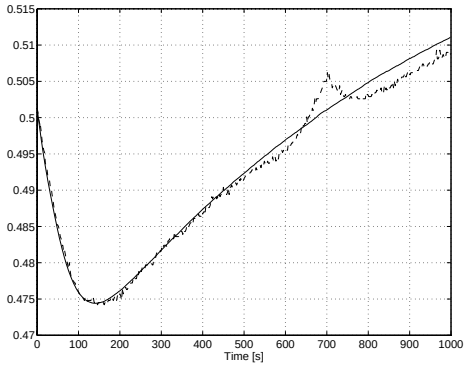

Fig. 65. Water level in the reservoir R_2 (h_2) in [m]; __ model; -- measurements

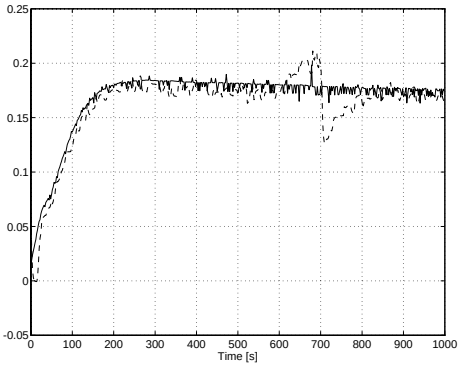

Fig. 68. Water flow Φ_2 through the valve V_2 in [l/s]; __ model, -- measurements

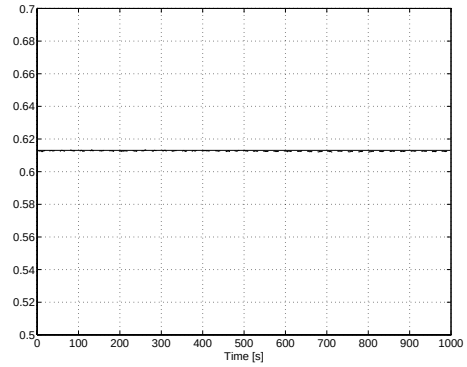

Fig. 66. The sum of water volumes in the separator R_1 and reservoir R_2 in [m^3]; __ model; -- measurements

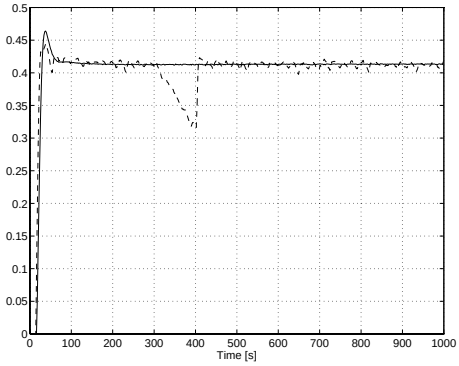

Fig. 69. Limited output of the pressure controller; __ model, -- measurements

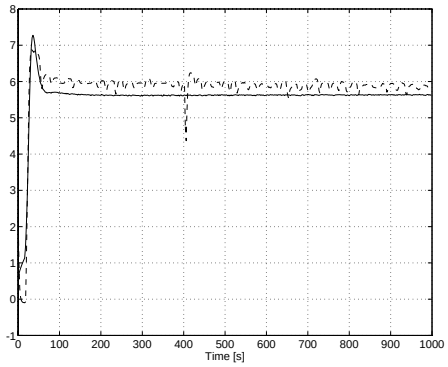

Fig. 67. Air flow Φ_1 through the valve V_1 in [l/s]; __ model, -- measurements

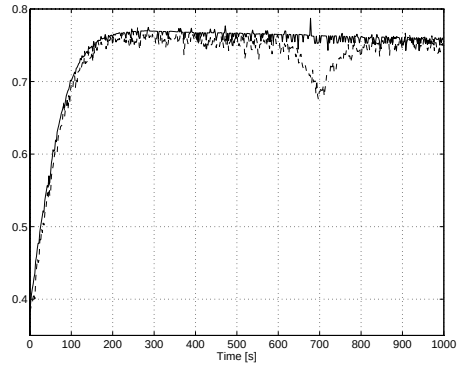

Fig. 70. Limited output of the level controller; __ model, -- measurements

5. Conclusions

Gas-liquid separator is one of several benchmark processes which will be used for testing and evaluation of different fault detection and isolation methods. In this work, a non-linear mathematical model of this semi-industrial process was developed. A linearised process model is proposed as well. The results of experiments show that both models satisfactory describes the process dynamics. The only problem which appeared in cross-validation is offset between measured and modelled water level in the separator. The reason is due to the fact that the final steady-state water level is very sensitive to the changes in valves positions. When comparing the closed-loop measured and modelled responses, the difference almost disappears.

Some improvements of the model can be done by carefully modelling valves characteristics. Some additional improvements could also be achieved by adding sensors for measuring air and water flows to the separator. The improvements are limited by unpredictable variations in supply voltage (220V AC) which changes the power of the pump and consequently has influence to the whole process response.

6. References

[1] Endress + Hauser, “Swingwirl II - Wirbeldurchflussmesser: Montage und Betriebsanleitung (the manual for the flow-meter)”

[2] F. G. Shinskey, “*Process Control Systems*”, 3rd edition, McGraw-Hill, pp. 135-143, 1988.

[3] D. Vrančić, Y. Peng, Đ. Juričić, “*Some Aspects and Design of Anti-Windup and Conditioned Transfer*”, Report DP-7169, Ljubljana, 1995.

7. Appendix

7.1 List of applied constants and variables

Constant	*Value*	*Unit*	*Description*
S_1	0.312	m^2	Cross-section area of R_1
S_2	0.32	m^2	Cross-section area of R_2
p_0	1.033	bar	Normal atmospheric pressure
ρ_0		kg/m^3	Air density at normal atmospheric pressure
h_{R1}	2.25	m	Height of the separator R_1
K_{01}	75.1	$l/(s \cdot bar^{1/2})$	Flow coefficient of valve V_1
R_1	46.1	-	The open-close flow ratio of valve V_1
K_{02}	0.742	$l/(s \cdot bar^{1/2})$	Flow coefficient of valve V_2
R_2	75.66	-	The open-close flow ratio of valve V_2
K_w	0.0981	bar/m	The proportional factor between the water level in [m] and pressure in [bar]
K_F	$1e^{-3}$	m^3/l	Proportional factor between the flow in m^3/s and l/s
Φ_w	0.1644	l/s	Water flow to the R_1
Φ_{air0}	6.46	l/s	Air flow to R_1 (at the atmospheric pressure)
Φ_{air1}	-1.615	l/(s·bar)	The proportional factor between air flow and pressure inside R_1
u_{2max}	0.8625	-	The maximum value of the variable v_2 (the position of V_2)
$\dot{v}_{max}$	0.66	s^{-1}	Maximum speed of valves opening
$\dot{v}_{min}$	-0.33	s^{-1}	Maximum speed of valves closing

Variable	*Unit*	*Description*
Φ_{air}	l/s	Air flow to the separator R_1
Φ_w	l/s	Water flow to the separator R_1
Φ_1	l/s	Air flow from the separator R_1
Φ_2	l/s	Water flow from the separator R_1
p_1	bar	Excess of gas pressure above the normal atmospheric pressure inside R_1
p	bar	Absolute air pressure inside R_1 $p=(p_0+p_1)$
p_{1s}	bar	Steady-state value of pressure p_1 used for linearisation
p_{V2s}	bar	Steady-state pressure on the valve V_2
h_1	m	Water level inside R_1
h_{1s}	m	Steady-state value of water level h_1 used for linearisation
h_2	m	Water level inside R_2
ρ	kg/m^3	Air density inside R_1
V	m^3	Gas volume inside R_1
m	kg	Mass of the gas inside R_1
v_1	-	Actual position of the valve V_1
Δv_1	-	Deviations from the steady-state $\Delta v_1=v_1-v_{1s}$ (used in linear model)
u_1	-	Valve command signal (desired position of V_1)
v_2	-	Actual position of valve V_2
Δv_2	-	Deviations from the steady-state $\Delta v_2=v_2-v_{2s}$ (used in linear model)
u_2	-	Valve command signal (desired position of V_2)
K_1	-	Proportional gain of the pressure controller
K_2	-	Proportional gain of the level controller
T_{i1}	-	Integral time constant of the pressure controller
T_{i2}	-	Integral time constant of the level controller

7.2 List of files

Measurements were taken by the program package LABTECH NOTEBOOK and are in the format of this program. First 6 lines are reserved for comments and the rest are measurements in ASCII format. The sampling time in all experiments is 1s.

File name	*Description*
LABXOL?.DAT	Open-loop response without faults; see Figures 13 to 17
LABXLOL?.DAT	Open-loop response for the linearised model without faults. Used measurements were those from 200 secs on; see Figures 31 to 35
LABXCL?.DAT	Closed-loop response without faults; see Figures 20 to 30
LABFACL?.DAT	Closed-loop response with actuator faults; see Figures 63 to 70
LABFBCL?.DAT	Closed-loop response with built-in faults; see Figures 43 to 51
LABFBOL?.DAT	Opened-loop response with built-in faults; see Figures 36 to 42
LABFSCL?.DAT	Closed-loop response with sensor faults; see Figures 53 to 61

The character ? stands for A, B or C and denotes the chosen measurement as follows:

Last character is A:

Column number	*Description*	
	Open-loop	*Closed-loop*
1	Time [s]	Time [s]
2	The valve1 command signal [-] (u_1)	The pressure p_1 reference [bar]
3	The pressure p_1 [bar]	The pressure p_1 [bar]
4	The valve2 command signal [-] (u_2)	The water level h_1 reference [m] for the closed-loop experiments
5	The level h_1 [m]	The level h_1 [m]

The last character is B (only for the closed-loop experiments):

Column number	***Description***
1	Time [s]
2	The unlimited pressure controller output [-]
3	The limited pressure controller output [-]
4	The unlimited level controller output [-]
5	The limited level controller output [-]

The last character is C:

Column number	***Description***
1	Time [s]
2	The air flow Φ_1 [l/s]
3	The water flow Φ_2 [l/s]
4	Digital signal from the LT_3 [-]
5	The level h_2 [m] (not available in all measurements)

Next MATLAB and SIMULINK files are also available:

Name of the file	***Description***
LINSCH.M	Scheme of the linearised process model in SIMULINK (see Fig. 12)
LINSCH1.M	The initialisation file in MATLAB for the LINSCH.M. Before starting, set the steady-state values p1s and h1s.
MODBLOCK.M	Scheme of the closed-loop configuration of the non-linear process model in SIMULINK (see Fig. 19)
MODVECT1.M	Scheme of the non-linear process model in SIMULINK (see Fig. 9)
DATA.MAT	Initialisation constants used in the process model